MEDICAL SCIENCE MONITOR BASIC RESEARCH

LABORATORY RESEARCH

e-ISSN 2325-4416
© Med Sci Monit Basic Res, 2020; 26: e928265
DOI: 10.12659/MSMBR.928265

Received: 2020.08.31
Accepted: 2020.11.16
Published: 2020.12.16

Paclitaxel Ameliorates Palmitate-Induced Injury in Mouse Podocytes

Authors' Contribution:
Study Design A
Data Collection B
Statistical Analysis C
Data Interpretation D
Manuscript Preparation E
Literature Search F
Funds Collection G

ABCDEF 1 Seung Seob Son
CDEF 1,2 Jeong Suk Kang
ACDEFG 1,2,3 Eun Young Lee

1 Department of Internal Medicine, Soonchunhyang University Cheonan Hospital, Cheonan, South Korea
2 Institute of Tissue Regeneration, College of Medicine, Soonchunhyang University, Cheonan, South Korea
3 Department of Internal Medicine, BK21 Four Project, College of Medicine, Soonchunhyang University, Cheonan, South Korea

Corresponding Author: Eun Young Lee, e-mail: eylee@sch.ac.kr
Source of support: This work was supported by the National Research Foundation (NRF) of Korea grant funded by the Korean government (Ministry of Science and ICT) (2020R1A2C2003438). It was also supported by the Soonchunhyang University Research Fund

Background: Palmitate, a common saturated free fatty acid, is increased in patients with diabetic nephropathy (DN). Excessive palmitate in kidney is known to cause proteinuria and fibrosis. Several studies have demonstrated that paclitaxel has anti-fibrotic and anti-inflammatory effects on kidney disease. However, whether paclitaxel can relieve podocyte injury is unclear.

Material/Methods: Immortalized mouse podocytes were used as an *in vitro* system. Palmitate was used to induce podocyte injury. Podocytes were divided into 4 groups: bovine serum albumin, palmitate, palmitate+1 nM paclitaxel, and palmitate+5 nM paclitaxel. The effects of paclitaxel on palmitate-induced podocyte injury were analyzed by western blot and real-time PCR. Intracellular reactive oxygen species (ROS) generation and podocyte cytoskeletons were analyzed using CM-H2DCF-DA and phalloidin staining.

Results: Paclitaxel restored downregulated expression of nephrin and synaptopodin and upregulated VEGF expression after injury induced by palmitate. Remarkably, palmitate-induced actin cytoskeleton rearrangement in podocytes was repaired by paclitaxel. Four endoplasmic reticulum stress markers, ATF-6α, Bip, CHOP, and spliced xBP1, were significantly increased in palmitate-treated podocytes compared with control podocytes. Such increases were decreased by paclitaxel treatment. Palmitate-induced ROS generation was ameliorated by paclitaxel. Elevated Nox4 expression was also improved by paclitaxel. Paclitaxel alleviated the expression levels of the antioxidant molecules, Nrf-2, HO-1, SOD-1, and SOD-2. The paclitaxel effects were accompanied by inhibition of the inflammatory cytokines, MCP-1, TNF-α, TNF-R2, and TLR4, as well as attenuation of the apoptosis markers, Bax, Bcl-2, and Caspase-3. Furthermore, paclitaxel suppressed the palmitate-induced fibrosis molecules, fibronectin and TGF-β1.

Conclusions: This study suggests that paclitaxel could be a therapeutic agent for treating palmitate-induced podocyte injury in DN.

MeSH Keywords: Paclitaxel • Palmitates • Podocytes

Full-text PDF: https://www.basic.medscimonit.com/abstract/index/idArt/928265

Indexed in: [Current Contents/Clinical Medicine] [SCI Expanded] [ISI Alerting System] [ISI Journals Master List] [Index Medicus/MEDLINE] [EMBASE/Excerpta Medica] [Chemical Abstracts/CAS]

Background

High accumulation of saturated free fatty acid (FFA) is one of various mechanisms that lead to type 2 diabetes and dyslipidemia. Palmitate is abundant in human plasma [1]. Levels of palmitate in those with type 2 diabetes are fourfold higher than those in normal adults [2]. FFA level is a major factor in chronic kidney disease (CKD), diabetes mellitus (DM) and obesity [3–6]. Excess FFA in the kidney contributes to podocyte damage through lipotoxicity pathways [7,8]. Palmitate causes inflammation, reactive oxygen species (ROS), endoplasmic reticulum (ER) stress, apoptosis, and actin cytoskeleton changes [7,9–11]. Previous studies have demonstrated that palmitate can induce podocyte injury, lead to glomerular damage, and increase proteinuria [5,10,12].

Podocytes are terminally differentiated epithelial cells of the glomerulus, and are components of the glomerular filtration barrier [13]. Each podocyte is composed of a cell body, major process, and foot processes. Podocytes also have specially slit diaphragms that function as intercellular junctions [14]. Podocyte damage is a key factor in glomerulosclerosis, and loss of podocytes can lead to proteinuria [15–17].

Paclitaxel, first extracted from the bark of the *Taxus brevifolia* tree, is the most important anti-cancer drug for breast, ovarian, stomach, and lung cancers [18]. Paclitaxel can stabilize microtubule polymers and interfere with microtubule disassembly, resulting in cell cycle arrest at the G0/G1 and G2/M phases, and cell death [19,20]. Recently, studies have shown that low-dose paclitaxel and high-dose paclitaxel exert their effects via different mechanisms [21]. Low-dose paclitaxel has effects on renal fibrosis and hepatic fibrosis through inhibition of TGF-β1/smad signaling [22,23]. In lipopolysaccharide (LPS)-induced acute lung injury and kidney injury models, paclitaxel has anti-inflammatory effects [24,25]. Moreover, low-dose paclitaxel can regenerate axons without causing injury to retina cells in rats [26]. Furthermore, paclitaxel has therapeutic effects for various non-cancer diseases.

Several studies have reported the effect of paclitaxel on kidney disease, using models including progressive glomerular damage and interstitial fibrosis using unilateral ureteral obstruction (UUO), remnant kidney model, and LPS-induced kidney injury model [27–30]. However, both the mechanism and the role of paclitaxel in kidney protection remain unclear.

Therefore, the objective of the present study was to investigate the therapeutic effect of paclitaxel on palmitate-induced podocyte injury. We found that paclitaxel had a therapeutic effect on palmitate-induced podocyte injury.

Material and Methods

Cell line and reagents

Conditionally immortalized mouse podocytes (kindly provided by Dr. Peter Mundel) [31] were propagated in collagen I (Sigma-Aldrich, St. Louis, MO, USA)-coated dishes. We used culture media composed of low glucose (5.5 mM) Dulbecco's modified Eagle's medium (Gibco, NY, USA) supplemented with 10% fetal bovine serum (FBS) (Gibco) or 5% FBS, 100 U/ml penicillin and 100 µg/ml streptomycin, at 2 different temperatures. At 33°C, podocytes were allowed to proliferate in the presence of 10 U/ml mouse recombinant interferon-γ (IFN-γ) (Sigma-Aldrich, St. Louis, MO, USA) to increase the expression of a thermosensitive T antigen. For the induction of differentiation, podocytes were cultured without IFN-γ for 14 days at 37°C.

Palmitate (Sigma-Aldrich) was used in conjugating fatty acid-free bovine serum albumin (BSA) (Sigma-Aldrich). We referred to the conjugating method of palmitate and BSA in a previously published paper [10]. Briefly, palmitate was dissolved in autoclaved distilled water and conjugated with 10% BSA. The cultured mouse podocytes were starved under serum-deprived conditions for 24 h [7] and treated with palmitate (300 µM) with or without paclitaxel (Sigma-Aldrich). The drug concentrations were 1 nM and 5 nM. Podocytes were treated with palmitate for 18 h or 24 h.

Measurement of reactive oxygen species generation

The amount of ROS from differentiated podocytes was measured using 2'-7' dichlorofluorescein diacetate (CM-H2DCF-DA, Invitrogen, New York, NY, USA). Briefly, after cells were treated with 10 µM CM-H2DCF-DA at 37°C for 30 min, cells were washed. Representative images and fluorescence intensity were analyzed using an LV10i inverted confocal microscope (Olympus, Tokyo, Japan) at a wavelength of 490 nm.

Assay for cell viability

To test for cell viability, we used the [3-(4,5-dimethylthiazol-2-yl)-2,5-diphenyl- tetrazolium bromide] MTT (Sigma-Aldrich, St. Louis, MO, USA) colorimetric assay. Differentiated podocytes were seeded into 24-well plates. After serum deprivation at 37°C for 24 h, podocytes were incubated with MTT (10 mg/ml) at 37°C for 4 h. After removing the supernatant, 130 µL dimethylsulfoxide (DMSO) was added to each well. After reaction for 20 min, the absorbance at 590 nm was measured on a microplate enzyme-linked immunosorbent assay (ELISA) reader (VICTOR™, X3, PerkinElmer, Seoul, Korea).

Indexed in: [Index Medicus/MEDLINE] [EMBASE/Excerpta Medica] [Chemical Abstracts/CAS]

Table 1. Sequences of primers used in this study.

Primer		Sequence
Nephrin	F	5'-GAG GAG GAT CGA ATC GAA TCA GGA A-3'
	R	5'-GGT CCA CTT CTG CTG TGC TA-3'
TNF-R2	F	5'-GTC GCG CTG GTC TTC GAA CTG-3'
	R	5'-GGT ATA CAT GCT TGC CTC ACA GTC-3'
TNF-α	F	5'-TCC CAG GTT CTC TTC TCT TCA AGG GA-3'
	R	5'-GGT GAG GAG CAC GTA GTC GG-3'
Nox4	F	5'-AAA AAT ATC ACA CAC TGA ATT CGA GAC T-3'
	R	5'-TGG GTC CAC AGC AGA AAA CTC-3'
Bip	F	5'-ACT TGG GGA CCA CCT ATT CC-3'
	R	5'-AGG AGT GAA GGC CAC ATA CG-3'
CHOP	F	5'-CAC CAC ACC TGA AAG CAG AA-3'
	R	5'-ATC CTC ATA CCA GGC TTC CA-3'
Spliced xBP1	F	5'-TGA GTC CGC AGC AGG TG-3'
	R	5'-GCA GAC TCT GGG GAA GGA C-3'
MCP-1	F	5'-CTG GAT CGG AAC CAA ATG AG-3'
	R	5'-CGG GTC AAC TTC ACA TTC AA-3'
HO-1	F	5'-ATC GTG CTC GCA TGA ACA CT-3'
	R	5'-CCA ACA CTG CAT TTA CAT GG-3'
SOD-1	F	5'-GCG TCA TTC ACT TCG AGC AGA-3'
	R	5'-GGA CCG CCA TGT TTC TTA GAG T-3'
SOD-2	F	5'-AGC CTC CCT GAC CTG CCT TA-3'
	R	5'-CGC CTC GTG GTA CTT CTC CT-3'
TLR4	F	5'-CCG CTT TCA CCT CTG CCT TCA C-3'
	R	5'-ACC ACA ATA ACC TTC CGG CTC TTG-3'
β-actin	F	5'-GGA CTC CTA TGT GGG T-3'
	R	5'-CTT CTC CAT GTC GTC GTC CCA GT-3'

Protein extraction and western blot

Podocytes were seeded onto 100 mm^2 cell culture plates, cultured, washed with cold phosphate buffered saline (PBS), and lysed with pro-prep (iNtRON, Seongnam-Si, Korea) containing a protease inhibitor cocktail (Roche Diagnostic GmbH, Mannheim, Germany). All cell lysates were quantified using the Bradford assay (Bio-Rad, Hercules, CA, USA) with BSA used as the standard. Equal amounts of proteins were separated by SDS-PAGE. The transferred membrane with the proteins was blocked with 5% nonfat dry milk at room temperature for 1 h and incubated with primary antibodies at 4°C overnight. To test ER stress, ROS, inflammation, apoptosis, and fibrosis, the membrane was incubated with primary antibodies against ATF-6α (Santa Cruz Biotechnology, Inc, Santa Cruz, CA, USA), Bip (Cell Signaling Technology, Danvers, MA, USA), TNF-R2 (Santa Cruz Biotechnology, Inc), TLR-4 (Santa Cruz Biotechnology, Inc), Nox4 (Santa Cruz Biotechnology, Inc), caspase-3 (Santa Cruz Biotechnology, Inc), Bax (Santa Cruz Biotechnology, Inc), Bcl-2 (Santa Cruz Biotechnology, Inc), fibronectin (Dako, an Agilent Technologies company, Carpinteria, CA), TGF-β1 (Santa Cruz Biotechnology, Inc), nephrin (Progen Biotechnik, Heidelberg, Germany), VEGF (Invitrogen Corporation, Carlsbad, CA, USA), synaptopodin (Synaptic Systems, Gottingen, Germany), and β-actin (Santa Cruz Biotechnology, Inc). After incubating with horseradish peroxidase-conjugated secondary antibodies against mouse (Promega Corporation, Madison, WI, USA), rabbit (Invitrogen), pig (Santa Cruz Biotechnology, Inc), and goat (Everest Biotech Ltd, Oxfordshire, UK) at room temperature for 3 h, the band was visualized with a ChemiDoc™ XRS+ (Biochemicals and Radiochemicals, Bio-Rad, Hercules, CA, USA) imaging system using electrochemiluminescent spray (Advansta, San Jose, CA, USA). The densities of the bands were analyzed using Image Labs (Bio-Rad Laboratories).

Indexed in: [Index Medicus/MEDLINE] [EMBASE/Excerpta Medica] [Chemical Abstracts/CAS]

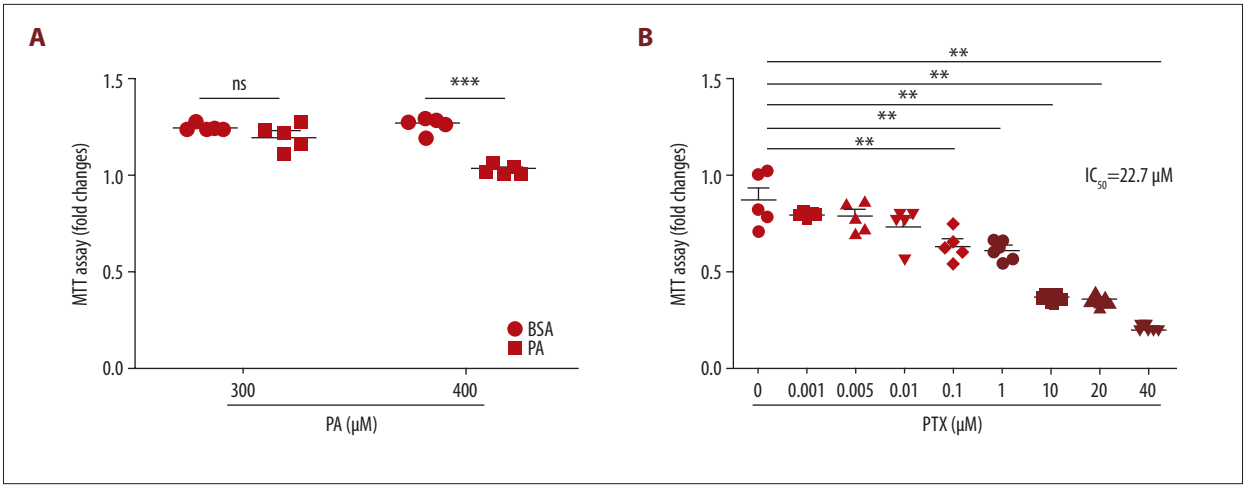

Figure 1. Effect of palmitate and paclitaxel on cell viability based on MTT assay. Cell viability was determined by MTT assay. (**A**) Mouse podocyte cells were incubated with 2 different concentrations of palmitate (300 μM and 400 μM) for 24 h. (**B**) Mouse podocyte cells were incubated with paclitaxel for 24 h at concentrations of 0–40 μM. IC50=22.7 μM. Error bars represent the mean±SEM (n=5). BSA – bovine serum albumin; PA – palmitate; PTX – paclitaxel. ** P<0.01 compared with control, *** P<0.001 compared with control.

Immunofluorescence for visualizing the actin cytoskeleton

Differentiated mouse podocytes were grown on coverslips with collagen coating, washed with PBS, and fixed with 3.7% paraformaldehyde in PBS at room temperature for 10 min. Podocytes were permeabilized with 0.2% Triton X-100 for 5 min, blocked with 1% BSA at room temperature for 1 h, and incubated with primary antibody against FITC-phalloidin (Sigma-Aldrich) at 4°C overnight. Coverslips with seeded podocytes were washed with PBS for 5 min and then stained with 4'-6-diamidino-2-phenylindole (DAPI) containing Vectashield mounting solution (Vector Laboratories, Burlingame, CA, USA). Actin cytoskeleton images were captured using an LV10i inverted confocal microscope (Olympus, Tokyo, Japan). To quantitatively analyze podocyte regeneration, we conducted Line receiver operating characteristic (ROC) analyses of the fluorescence intensity for each picture [10]. The area under the receiver operating characteristics curve (AUC) graph was quantified using the ImageJ program (developed at the National Institutes of Health; NIH, Bethesda, MD, USA) and the Laboratory for Optical and Computational Instrumentation (LOCI, University of Wisconsin, Madison, WI, USA).

RNA extraction and real-time quantitative PCR

According to the manufacturer's instructions, total RNA was extracted from mouse podocytes using TRIzol (Ambion Inc, Austin, TX, USA). cDNA was prepared from 1 μg of total RNA using a ReverTra Ace qPCR RT master mix (Toyobo, Osaka, Japan). Quantitative real-time PCR was conducted using SYBR Green PCR master mix (TOYOBO, San Jose, CA, USA) and analyzed with the CFX connect real-time system (Bio-Rad, Hercules, CA, USA). The mRNA expression of podocyte markers, ER stress markers, antioxidant markers, and inflammatory cytokines was quantitatively analyzed by quantitative real-time PCR using sequence-specific mouse primers (Table 1). β-actin was used as housekeeping gene. Data were analyzed via the 2–ΔΔCt method.

Statistical analysis

All experiments were repeated at least 3 times under the same conditions (n=3–5). The data were expressed as mean±standard error of the mean (SEM). The results were analyzed using one-way analysis of variance (ANOVA) for multiple comparisons among the multiple groups and the post-hoc Newman-Keuls test. Differences with values of P<0.05 were considered significant.

Results

Cytotoxicity effects of paclitaxel and palmitate

The cytotoxicity levels of palmitate and paclitaxel were determined using MTT assay. Palmitate at 400 μM had significant toxic effects on podocytes (Figure 1A). Therefore, 300 μM palmitate was used to induce podocyte injury. As shown in Figure 1B, 100nM paclitaxel resulted in significant toxic effects on mouse podocyte cell viability. However, paclitaxel showed no cytotoxicity to podocytes at 1 nM and 5 nM concentration. The 50% growth inhibitory concentration (IC50) value for paclitaxel was 22.7 μM.

Indexed in: [Index Medicus/MEDLINE] [EMBASE/Excerpta Medica] [Chemical Abstracts/CAS]

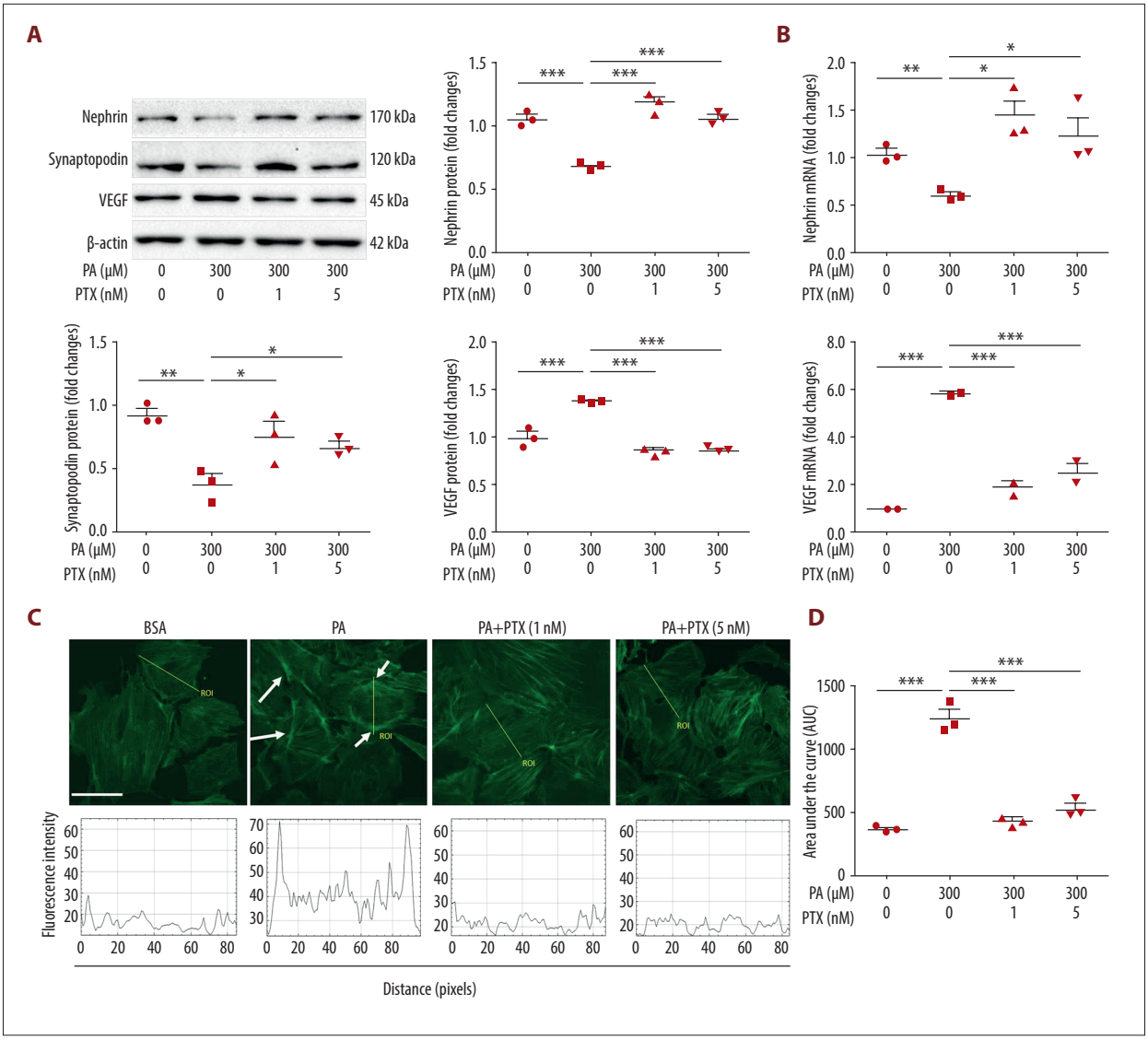

Figure 2. Effect of paclitaxel treatment on palmitate-induced podocyte damage. Mouse podocyte cells were treated with 300 μM palmitate with or without paclitaxel for 24 h. (**A**) Western blots and densitometry for nephrin, synaptopodin, and VEGF. (**B**) Real-time PCR for nephrin and VEGF was normalized by β-actin mRNA level in the same sample. (**C**) FITC-phalloidin staining showing F-actin. Arrows indicate reorganization of F-actin. Line ROC analyses of the fluorescence intensity for each picture are shown at the bottom. Quantification was performed as in [10]. (**D**) Area under the curve analysis of the results shown in (**C**). Error bars represent the mean±SEM (*n*=3). Magnification 40×; bar=60 μm. BSA – bovine serum albumin; PA – palmitate; PTX – paclitaxel: ROC – receiver operating characteristic. * $P<0.05$, ** $P<0.01$, *** $P<0.001$ compared with palmitate.

Paclitaxel ameliorates palmitate-induced podocyte damage

The expression of nephrin and synaptopodin was decreased in palmitate-treated podocytes compared with BSA-treated control podocytes. However, expression was increased in paclitaxel-cotreated podocytes. Upregulation of VEGF expression in palmitate-treated podocytes was restored by paclitaxel-cotreated podocytes (Figure 2A). Similarly, downregulated expression of nephrin mRNA and upregulated expression of VEGF mRNA in palmitate-treated podocytes were recovered by paclitaxel (Figure 2B). To confirm the effect of paclitaxel on the actin cytoskeleton, we observed structural changes in F-actin in palmitate-treated podocytes with or without paclitaxel. The results showed podocyte rearrangement caused by palmitate. However, paclitaxel-cotreated podocytes recovered these changes compared with the control (Figure 2C, 2D). To measure fluorescence intensity, we used line ROC analysis. The BSA-treated cells had well-arranged fluorescence intensity

Indexed in: [Index Medicus/MEDLINE] [EMBASE/Excerpta Medica] [Chemical Abstracts/CAS]

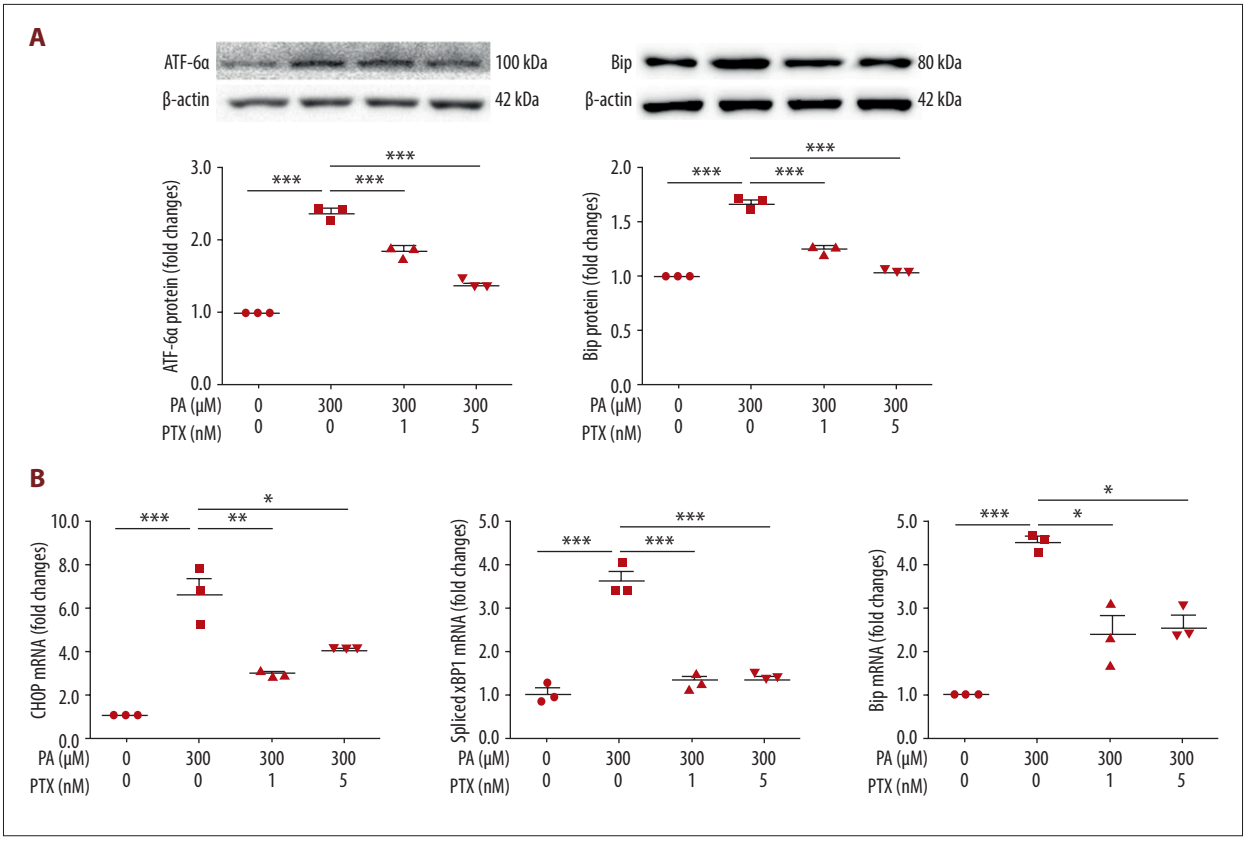

Figure 3. Effect of paclitaxel on palmitate-induced ER stress. Podocytes were treated with 300 μM palmitate with or without paclitaxel for 24 h. (**A**) Western blots (**top**) and densitometry (**bottom**) for ATF-6α and Bip. (**B**) Real-time PCR for CHOP, spliced XBP1, and Bip was normalized by β-actin mRNA level in the same sample. Error bars represent the mean±SEM. (*n*=3). BSA – bovine serum albumin; PA – palmitate; PTX – paclitaxel. * *P*<0.05, ** *P*<0.01, *** *P*<0.001 compared with palmitate.

around stress fibers in the cytosol. The palmitate-treated cells showed high fluorescence intensity in the cortical region, but the paclitaxel-treated cells showed fluorescence intensity similar to that in the BSA-treated cells.

Paclitaxel reduces palmitate-induced endoplasmic reticulum stress

To test the effect of paclitaxel on ER stress, we measured ER stress markers. Expression levels of ATF-6α and Bip were increased in palmitate-treated podocytes compared with those in the BSA-treated control (Figure 3A). However, paclitaxel-cotreated podocytes showed reduced expression of ATF-6α and Bip (paclitaxel at 1 nM and 5 nM). Palmitate increased mRNA levels of CHOP, spliced XBP1, and Bip. Such increases were improved by paclitaxel (Figure 3B).

Paclitaxel ameliorates palmitate-induced reactive oxygen species and restores antioxidant molecules

ROS is a factor in podocyte damage and degeneration in CKD. To test the effect of paclitaxel on ROS generation, we measured ROS using CM-H2DCF-DA. As shown in Figure 4B and 4C, palmitate increased intracellular ROS accumulation whereas paclitaxel ameliorated ROS generation. To determine whether palmitate-induced ROS generation was associated with NADPH oxidase (NOX), we analyzed Nox4 expression using western blot. Nox4 was significantly increased in palmitate-treated podocytes compared with BSA-treated control podocytes. This increase was effectively attenuated by paclitaxel (Figure 4A). We checked the effect of paclitaxel on antioxidant molecules via palmitate-induced downregulation of Nrf-2. Such downregulation was recovered by paclitaxel (Figure 4A). Total mRNA expression levels of HO-1, SOD1, and SOD2 were decreased in palmitate-treated podocytes. Such decreases were significantly restored by paclitaxel (Figure 4D).

Paclitaxel attenuates palmitate-induced inflammation

To assess the effect of paclitaxel on inflammation, we investigated the expression of inflammation molecules. In the palmitate-treated podocytes, mRNA levels of TNF-α and MCP-1 were increased compared with those in the BSA-treated controls. Such increases were significantly attenuated in paclitaxel-cotreated podocytes (Figure 5A). Palmitate-induced TLR4

Indexed in: [Index Medicus/MEDLINE] [EMBASE/Excerpta Medica] [Chemical Abstracts/CAS]

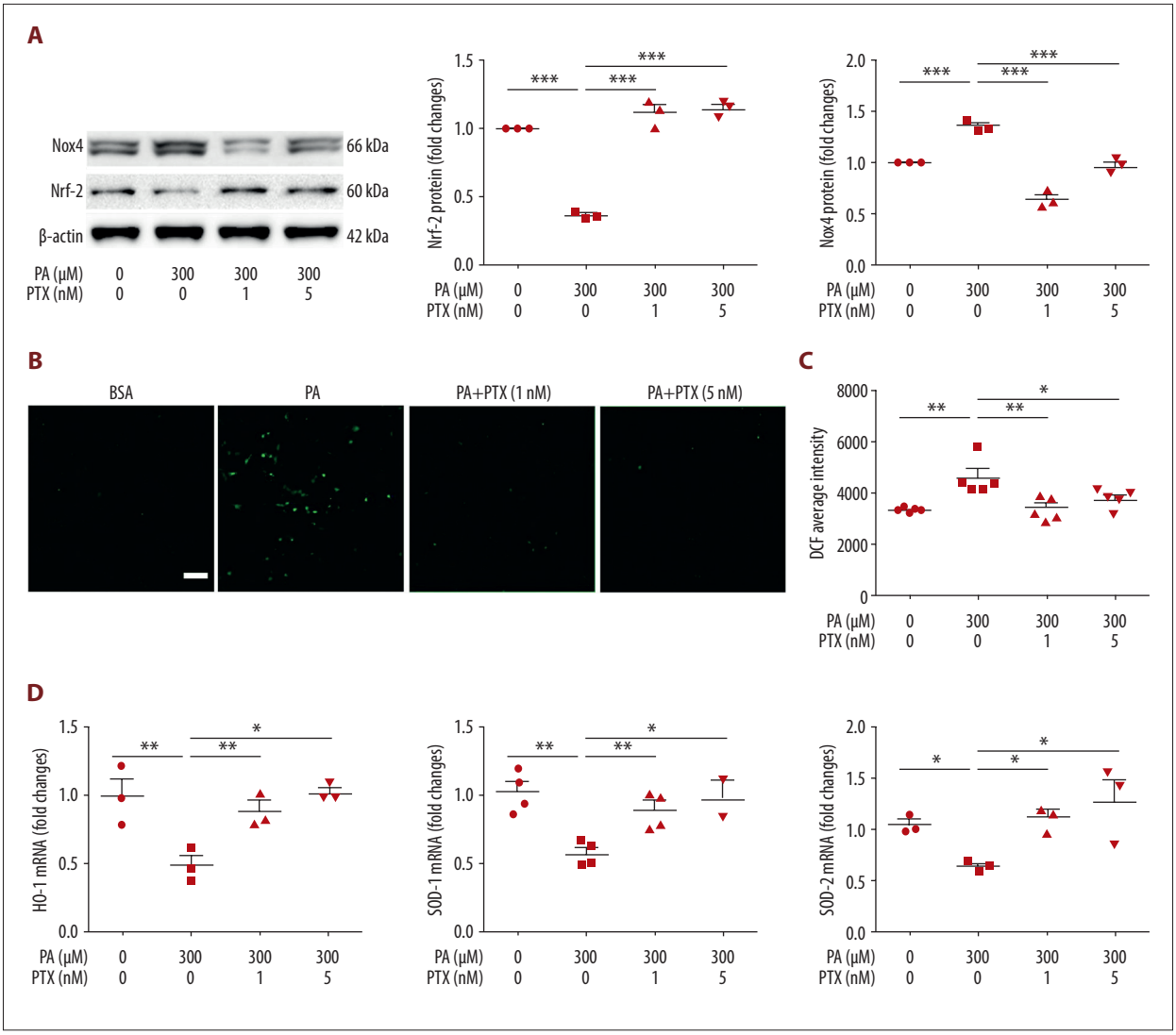

Figure 4. Effect of paclitaxel on palmitate-induced reactive oxygen species and antioxidant molecules. (**A**) Western blot (**left**) and densitometry (**right**) showing Nox4 and Nrf-2 expression. Error bar represents the mean±SEM (n=3) (B) Representative images of palmitate-induced dichlorofluorescein fluorescence (DCF). Podocytes were treated with 300 μM palmitate with or without paclitaxel for 18 h, and 10 μM of CM-H2DCF-DA was used for treatment at 37°C for 30 min. Bar=200 μm. (**C**) Histogram analysis of the results shown in (**B**). Error bar represents the mean±SEM (n=5). (**D**) Real-time PCR of HO-1, SOD-1, and SOD-2 was normalized by β-actin mRNA level in the same sample. Error bar represents the mean±SEM (n=3). BSA – bovine serum albumin; PA – palmitate; PTX – paclitaxel. * P<0.05, ** P<0.01, *** P<0.001 compared with palmitate.

and TNF-R2 protein and mRNA expression levels were also restored by paclitaxel (Figure 5B).

Paclitaxel recovers palmitate-induced apoptosis and fibrosis molecules

To investigate the effect of paclitaxel on apoptosis, we performed western blot analysis. Expression levels of bax and caspase-3 proteins were increased by palmitate but decreased by paclitaxel. Bcl-2 was downregulated by palmitate. Such downregulation was recovered by paclitaxel (Figure 6A). To assess the effect of paclitaxel on palmitate-induced fibrosis, TGF-β1 and fibronectin levels were evaluated using western blot. As shown in Figure 6B, levels of these proteins in palmitate-treated podocytes were increased compared with those in BSA-treated controls. However, TGF-β1 and fibronectin were downregulated by paclitaxel.

Discussion

CKD is caused by glomerular damage with diabetic nephropathy (DN) [2–4]. Sun et al. have reported that the progression

Indexed in: [Index Medicus/MEDLINE] [EMBASE/Excerpta Medica] [Chemical Abstracts/CAS]

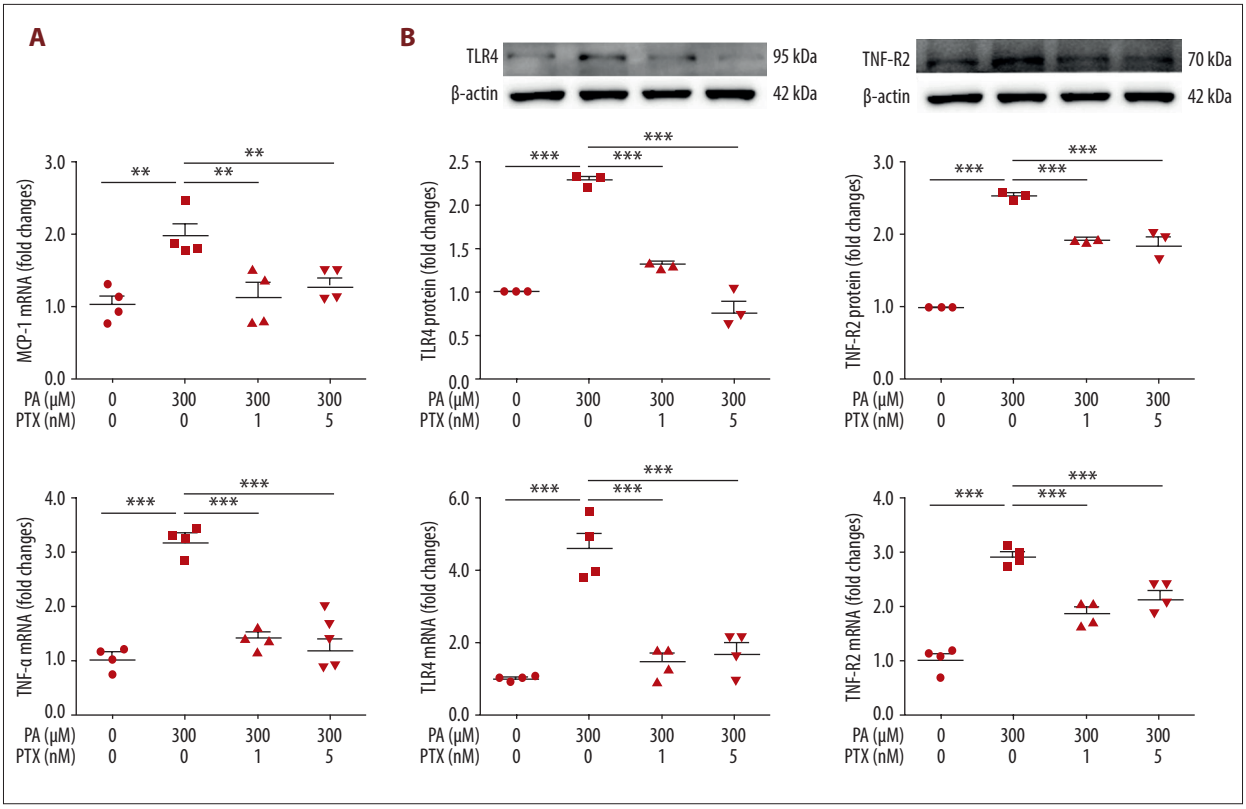

Figure 5. Effect of paclitaxel on palmitate-induced inflammation. Podocytes were treated with 300 μM palmitate with or without paclitaxel for 24 h. (**A**) Real-time PCR of MCP-1 (**top**) and TNF-α (**bottom**) were normalized by β-actin mRNA level in the same sample. Error bar represents the mean±SEM (n=4). (**B**) TNF-R2 and TLR4 mRNA was normalized by β-actin mRNA level in the same sample. Western blots, densitometry (**top**, n=3) and mRNA expression are shown (**bottom**, n=4). Bar represent the mean±SEM. BSA – bovine serum albumin; PA – palmitate; PTX – paclitaxel. ** P<0.01, *** P<0.001 compared with palmitate.

of renal disease associated with 5/6 nephrectomy [22], a well-known CKD model, is protected by paclitaxel; paclitaxel therefore plays important roles in kidney protection. Paclitaxel, one of many cancer-targeting drugs, has also emerged as a treatment for kidney fibrosis and proteinuria [22]. Zhang et al. [24,29] have reported that paclitaxel exerts its effects in UUO models by inhibiting TGF-β1/smad signaling and STAT3 signaling. Paclitaxel has effects on nephrectomy models and UUO models of CKD. In paclitaxel studies of kidney disease, there are still only CKD models and inflammation-related LPS-induced models. However, the efficacy and mechanism of paclitaxel have not been reported for DN. In this study, we investigated the effect of paclitaxel on podocyte injury in DN.

Martínez-García et al. [7] reported that VEGF expression is upregulated in podocytes damaged by palmitate. Chavez-Tapia et al. [32] have demonstrated that VEGF expression is increased in hepatic cells cotreated with palmitic and oleic acids. Similarly, our results showed that the expression of VEGF was increased in palmitate-treated podocytes. Paclitaxel-cotreated podocytes showed improved VEGF expression. It has been reported that nephrin gene expression is impaired in palmitate-treated podocytes [7]. Consistently with this result, our results also showed that palmitate treatment damaged the slit diaphragm protein nephrin. Sun et al. [33] have shown that palmitate can decrease synaptopodin in podocytes. We also observed lowered expression of synaptopodin after palmitate treatment. However, paclitaxel improved its expression. Our results also showed that palmitate caused changes in the actin cytoskeleton which rearranged focal adhesion to the parietal site. However, paclitaxel minimized this remodeling of the actin cytoskeleton caused by palmitate.

We investigated ER stress associated with lipid accumulation in podocytes. Madhusudhan et al. [34] have shown that ER responses associated with ATF-6α, CHOP, and spliced XBP1 signaling are increased in DN. Xu et al. [10] have demonstrated that palmitate-treated podocytes not only show increased levels of the ER stress markers, CHOP and GRP78, but also show upregulated CHOP, phosphorylated eIF2α, phosphorylated PERK, and spliced XBP1. Our results also showed that palmitate-treated podocytes had increases in ER stress markers, including ATF-6α, Bip, CHOP, and spliced XBP1. However, paclitaxel markedly restored these ER stress markers.

Indexed in: [Index Medicus/MEDLINE] [EMBASE/Excerpta Medica] [Chemical Abstracts/CAS]

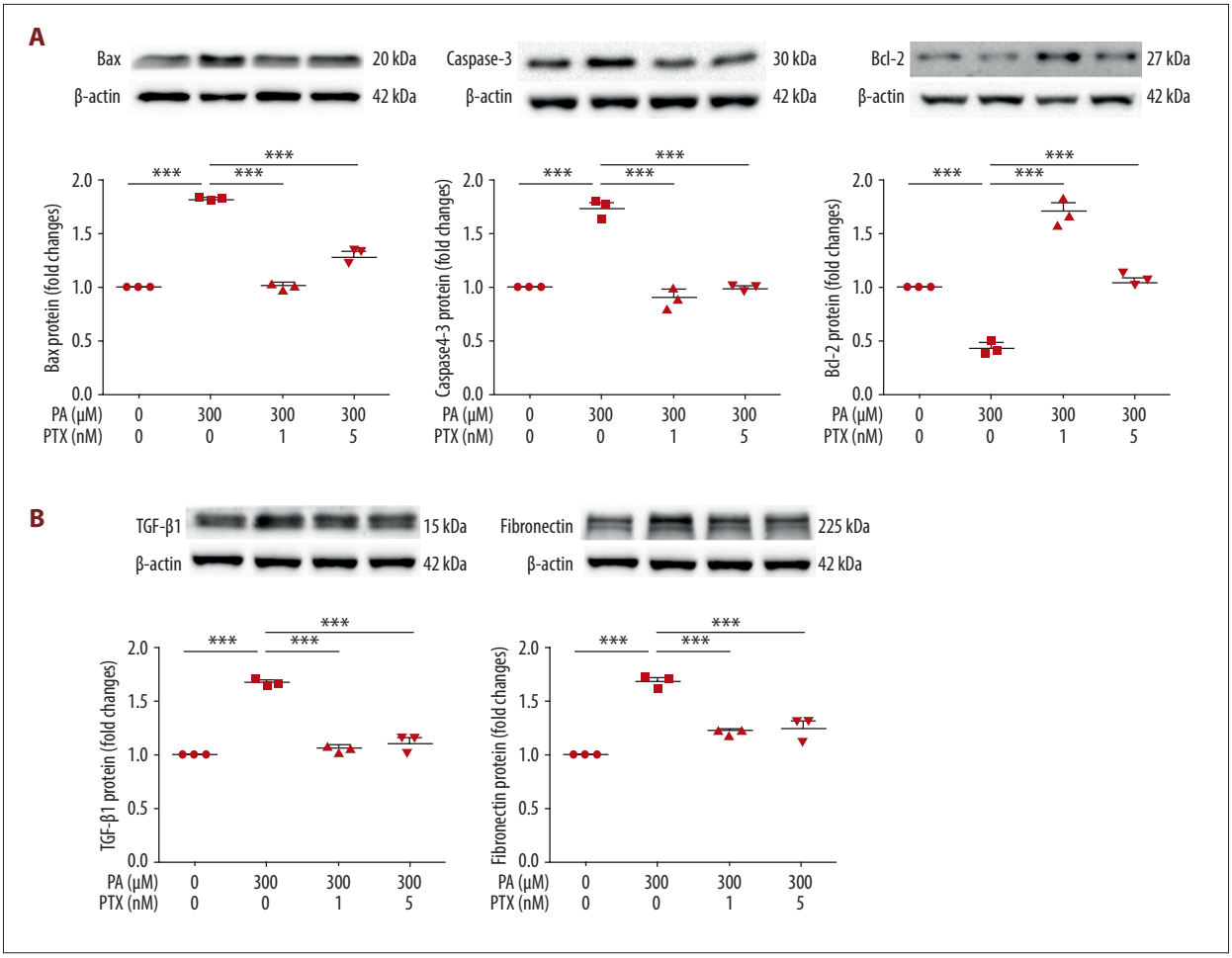

Figure 6. Effect of paclitaxel on palmitate-induced apoptosis and fibrosis molecules. Podocytes were treated with 300 μM palmitate with or without paclitaxel for 18 h. (**A**) Western blot (**top**) and densitometry (**bottom**) for Bax, Caspase-3, and Bcl-2 demonstrating that palmitate-induced apoptosis was restored by paclitaxel. (**B**) Western blot (**top**) and densitometry (**bottom**) for fibronectin and TGF-β1, estimating that palmitate-induced apoptosis was restored by paclitaxel. Error bars represent the mean±SEM (n=3). BSA – bovine serum albumin; PA – palmitate; PTX – paclitaxel. *** P<0.001 compared with palmitate.

Palmitate is known to increase ROS levels in db/db (diabetic dyslipidemia) mouse podocytes [35]. Han et al. [36] have demonstrated that NADPH oxidase 4 (Nox4) and ROS production are increased in palmitate- and glucose-cotreated adipocytes. Excess palmitate can induce endothelial dysfunction by Nox4 in human umbilical vein endothelial cells. Our results showed that ROS production and Nox4 upregulation in palmitate-treated podocytes were decreased in paclitaxel-cotreated podocytes. Furthermore, antioxidant molecules such as Nrf-2, HO-1, SOD1, and SOD2 were decreased in palmitate-treated podocytes whereas paclitaxel restored them.

Inflammatory markers such as MCP-1 and TNF-α are upregulated in high glucose-treated podocytes and other tissues [37,38]. Expression levels of IL-6, MCP-1, TNF-α, and TLR-4 are increased in palmitate-treated podocytes [7]. Our results showed that levels of TNF-α, MCP-1, and TLR-4 associated with inflammation were activated by palmitate. Levels of these same molecules were recovered by paclitaxel treatment.

Retinal pericytes and insulinoma cells treated with palmitate show upregulation of apoptosis. Palmitate not only increases Bax and caspase-3 expression, but also decreases Bcl-2 expression [39–41]. Our results confirmed that increases in Bax and caspase-3 protein in palmitate-treated podocytes were ameliorated by paclitaxel. In addition, paclitaxel recovered Bcl-2 protein decreases induced by palmitate.

Palmitate is known to induce cell apoptosis, but also to activate fibrotic molecules in cardiac h9c2 cells [39]. Collagen I, α-SMA, and fibronectin are increased in podocytes in DN [42,43]. Our results demonstrated that palmitate stimulation enhanced fibronectin and TGF-β1 expression in podocytes while paclitaxel significantly restored the expression of these molecules.

Indexed in: [Index Medicus/MEDLINE] [EMBASE/Excerpta Medica] [Chemical Abstracts/CAS]

Conclusions

Our results suggest that paclitaxel can ameliorate podocyte injury by improving ER stress, oxidative stress, inflammation, and fibrosis as well as by improving the actin cytoskeleton. Therefore, paclitaxel might be a novel therapeutic target for DN.

Conflict of interest

None.

References:

1. Richieri GV, Kleinfeld AM: Unbound free fatty acid levels in human serum. J Lipid Res, 1995; 36(2): 229–40
2. Van der Vusse GJ, Roemen TH: Gradient of fatty acids from blood plasma to skeletal muscle in dogs. J Appl Physiol (1985), 1995; 78(5): 1839–43
3. Hall ME, do Carmo JM, da Silva AA et al: Obesity, hypertension, and chronic kidney disease. Int J Nephrol Renovasc Dis, 2014; 7: 75–88
4. Wild S, Roglic G, Green A et al: Global prevalence of diabetes: Estimates for the year 2000 and projections for 2030. Diabetes Care, 2004; 27(5): 1047–53
5. Abboud H, Henrich WL: Clinical practice. Stage IV chronic kidney disease. N Engl J Med, 2010; 362(1): 56–65
6. Ising C, Koehler S, Brähler S et al: Inhibition of insulin/IGF-1 receptor signaling protects from mitochondria-mediated kidney failure. EMBO Mol Med, 2015; 7(3): 275–87
7. Martínez-García C, Izquierdo-Lahuerta A, Vivas Y et al: Renal lipotoxicity-associated inflammation and insulin resistance affects actin cytoskeleton organization in podocytes. PloS One, 2015; 10(11): e0142291
8. Alpers CE, Hudkins KL: Pathology identifies glomerular treatment targets in diabetic nephropathy. Kidney Res Clin Pract, 2018; 37(2): 106–11
9. Sieber J, Lindenmeyer MT, Kampe K et al: Regulation of podocyte survival and endoplasmic reticulum stress by fatty acids. Am J Physiol Renal Physiol, 2010; 299(4): F821–29
10. Xu S, Nam SM, Kim JH et al: Palmitate induces ER calcium depletion and apoptosis in mouse podocytes subsequent to mitochondrial oxidative stress. Cell Death Dis, 2015; 6(11): e1976
11. Lennon R, Pons D, Sabin MA et al: Saturated fatty acids induce insulin resistance in human podocytes: Implications for diabetic nephropathy. Nephrol Dial Transplant, 2009; 24(11): 3288–96
12. Tsun JG, Yung S, Chau MK et al: Cellular cholesterol transport proteins in diabetic nephropathy. PLoS One, 2014; 9(9): e105787
13. Michaud JL, Kennedy CR: The podocyte in health and disease: Insights from the mouse. Clin Sci (Lond), 2007; 112(6): 325–35
14. Leeuwis JW, Nguyen TQ, Dendooven A et al: Targeting podocyte-associated diseases. Adv Drug Deliv Rev, 2010; 62(14): 1325–36
15. Mundel P, Shankland SJ: Podocyte biology and response to injury. J Am Soc Nephrol, 2002; 13(12): 3005–15
16. Pavenstädt H, Kriz W, Kretzler M: Cell biology of the glomerular podocyte. Physiol Rev, 2003; 83(1): 253–307
17. Li X, Zhang X, Li X et al: The role of survivin in podocyte injury induced by puromycin aminonucleoside. Int J Mol Sci, 2014; 15(4): 6657–73
18. Zhang D, Yang R, Wang S et al: Paclitaxel: New uses for an old drug. Drug Des Devel Ther, 2014; 8: 279–84
19. Bharadwaj R, Yu H: The spindle checkpoint, aneuploidy, and cancer. Oncogene, 2004; 23(11): 2016–27
20. Brito DA, Yang Z, Rieder CL: Microtubules do not promote mitotic slippage when the spindle assembly checkpoint cannot be satisfied. J Cell Biol, 2008; 182(4): 623–29
21. Ganguly A, Yang H, Cabral F: Paclitaxel-dependent cell lines reveal a novel drug activity. Mol Cancer Ther, 2010; 9(11): 2914–23
22. Sun L, Zhang D, Liu F et al: Low-dose paclitaxel ameliorates fibrosis in the remnant kidney model by down-regulating miR-192. J Pathol, 2011; 225(3): 364–77
23. Zhou J, Zhong DW, Wang QW et al: Paclitaxel ameliorates fibrosis in hepatic stellate cells via inhibition of TGF-beta/Smad activity. World J Gastroenterol, 2010; 16(26): 3330–34
24. Zhang D, Sun L, Xian W et al: Low-dose paclitaxel ameliorates renal fibrosis in rat UUO model by inhibition of TGF-beta/Smad activity. Lab Invest, 2010; 90(3): 436–47
25. Mirzapoiazova T, Kolosova IA, Moreno L et al: Suppression of endotoxin-induced inflammation by taxol. Eur Respir J, 2007; 30(3): 429–35
26. Sengottuvel V, Leibinger M, Pfreimer M et al: Taxol facilitates axon regeneration in the mature CNS. J Neurosci, 2011; 31(7): 2688–99
27. Zhang D, Li Y, Liu Y et al: Paclitaxel ameliorates lipopolysaccharide-induced kidney injury by binding myeloid differentiation protein-2 to block Toll-like receptor 4-mediated nuclear factor-κB activation and cytokine production. J Pharmacol Exp Ther, 2013; 345(1): 69–75
28. Karbalay-Doust S, Noorafshan A, Pourshahid SM: Taxol and taurine protect the renal tissue of rats after unilateral ureteral obstruction: A stereological survey. Korean J Urol, 2012; 53(5): 360–67
29. Zhang L, Xu X, Yang R et al: Paclitaxel attenuates renal interstitial fibroblast activation and interstitial fibrosis by inhibiting STAT3 signaling. Drug Des Devel Ther, 2015; 9: 2139–48
30. Jung ES, Lee J, Heo NJ et al: Low-dose paclitaxel ameliorates renal fibrosis by suppressing transforming growth factor-β1-induced plasminogen activator inhibitor-1 signaling. Nephrology (Carlton), 2016; 21(7): 574–82
31. Shankland SJ, Pippin JW, Reiser J: Podocytes in culture: Past, present, and future. Kidney Int, 2007; 72: 26–36
32. Chavez-Tapia NC, Rosso N, Tiribelli C: Effect of intracellular lipid accumulation in a new model of non-alcoholic fatty liver disease. BMC Gastroenterol, 2012; 12: 20
33. Sun YB, Qu X, Howard V et al: Smad3 deficiency protects mice from obesity-induced podocyte injury that precedes insulin resistance. Kidney Int, 2015; 88(2): 286–98
34. Madhusudhan T, Wang H, Dong W et al: Defective podocyte insulin signalling through p85-XBP1 promotes ATF6-dependent maladaptive ER-stress response in diabetic nephropathy. Nat Commun, 2015; 6: 6496
35. Gao D, Nong S, Huang X et al: The effects of palmitate on hepatic insulin resistance are mediated by NADPH Oxidase 3-derived reactive oxygen species through JNK and p38MAPK pathways. J Biol Chem, 2010; 285(39): 29965–73
36. Han CY, Umemoto T, Omer M et al: NADPH oxidase-derived reactive oxygen species increases expression of monocyte chemotactic factor genes in cultured adipocytes. J Biol Chem, 2012; 287(13): 10379–93
37. Hivert MF, Sullivan LM, Fox CS et al: Associations of adiponectin, resistin, and tumor necrosis factor-alpha with insulin resistance. J Clin Endocrinol Metab, 2008; 93(8): 3165–72
38. Schenk S, Saberi M, Olefsky JM: Insulin sensitivity: Modulation by nutrients and inflammation. J Clin Invest, 2008; 118(9): 2992–3002
39. Zhong P, Quan D, Peng J et al: Role of CaMKII in free fatty acid/hyperlipidemia-induced cardiac remodeling both *in vitro* and *in vivo*. J Mol Cell Cardiol, 2017; 109: 1–16
40. Simon-Szabó L, Kokas M, Mandl J et al: Metformin attenuates palmitate-induced endoplasmic reticulum stress, serine phosphorylation of IRS-1 and apoptosis in rat insulinoma cells. PLoS One, 2014; 9(6): e97868
41. Cacicedo JM, Benjachareowong S, Chou E et al: Palmitate-induced apoptosis in cultured bovine retinal pericytes: Roles of NAD(P)H oxidase, oxidant stress, and ceramide. Diabetes, 2005; 54(6): 1838–45
42. Li N, Zhang J, Yan X et al: SIRT3-KLF15 signaling ameliorates kidney injury induced by hypertension. Oncotarget, 2017; 8(24): 39592–604
43. Yoon SY, Xu ZG, Ryu DR et al: The Effect of Pioglitazone on the Expression of Transforming Growth Factor (TGF)-β1 and fibronectin in diabetic nephropathy. Kidney Res Clin Pract, 2006; 25(3): 353–64

Indexed in: [Index Medicus/MEDLINE] [EMBASE/Excerpta Medica] [Chemical Abstracts/CAS]